An Alternate Analysis for the Second-Order High Frequency Bistatic Radar Cross Section of the Ocean Surface – Patch Scatter and its Inversion

Eric Gill, *Member, IEEE*, Weimin Huang, Jianjun Zhang
Faculty of Engineering and Applied Science, Memorial University of Newfoundland, St. John's, Newfoundland, A1B 3X5, Canada
Email: egill@engr.mun.ca

Abstract— **In this paper, the verification of the second-order high frequency (HF) ocean surface cross section for a surface patch remote from the transmitter and receiver is presented. The bistatic result is shown to reduce to the proper monstatic models when the appropriate geometry for backscatter is introduced. In particular, the electromagnetic coupling coefficient for the bistatic case is seen to incorporate its monostatic counterpart. It is well-known that the second order portion of the HF radar spectrum of the ocean echo contains substantial information on the surface gravity wave spectrum. Thus, the initial analysis forms the basis for the extraction of ocean surface parameters from bistatic HF radar data. An inversion technique for extraction of ocean surface wave parameters from bistatic HF radar data is briefly developed here. The inversion results from simulated spectra are seen to be very reasonable.**

I. INTRODUCTION

While several decades have elapsed in the significant application of high frequency (HF) surface wave radar to remote sensing in the ocean environment (see, for example, [1]-[3]), work continues on several related fronts. One of these involves the scattering analysis required to address the bistatic problem in which the transmitter and receiver are far removed from each other. A comprehensive investigation leading to bistatic cross sections of the ocean surface appears in [4]-[5]. The work there accounts for the fact that both radar sites may be surrounded or nearly surrounded by water. This leads to components of scatter which significantly complicate the modeling analysis beyond what is necessary if the transmitter and receiver operate from a shoreline with the ocean existing only in front of the radar components. Here, we consider a new approach to the the latter case, so that the scattering from a patch of ocean far removed from both the transmit and receive sites forms the most significant portion of the received second-order energy. In Section II, it is shown that this so-called bistatic "patch scatter" cross section reduces exactly to the monostatic case when the appropriate geometry is introduced into the models. An inversion technique similar to that suggested in [6] for the monostatic case is examined for its applicability to the extraction of wave information from bistatically operated radars in Section III. The results from simulations are discussed in Section IV, followed by a few concluding remarks.

II. Theoretical Verification of Cross Section

A. The Complete Equation Form

It has been shown [4] that the double-scatter field from HF radiation impinging the ocean surface consists of three significant terms: (1) two scatters occur on a patch of surface remote from both the transmitter and receiver (the patch being the same as that for the single, first-order scatter); (2) a single scatter near the transmitter is followed by another on the remote patch before reception; and (3) a first scatter on the remote patch is followed by another at the receiver immediately prior to reception. As to the patch scattering which is an asymptotic two-dimensional double-convolution, Gill and Walsh [5] carried out the inner convolution after its gradient. The second order radar cross section for patch scatter relevant to this work results from carrying out the convolution before taking the gradient and is given in [7] as

$$\begin{aligned}\sigma_{2P}(\omega_d) \;=\; & 2^3\pi K_0^2 \sum_{m_1=\pm1}\sum_{m_2=\pm1}\int_{-\infty}^{\infty}\int_{-\pi}^{\pi}\int_{-\infty}^{\infty} S(m_1\vec{K}_1)\\ & \cdot S(m_2)\vec{K}_2|\Gamma_P|^2 K_{rs}^2\cos\phi_0\\ & \cdot\Delta\rho_{s21} Sa^2\left[\frac{\Delta\rho_{s21}}{2}\left(\frac{K_{rs}}{\cos\phi_0}-2K_0\right)\right]\\ & \cdot\delta(\omega_d+m_1\sqrt{gK_1}+m_2\sqrt{gK_2})\\ & \cdot K_1 dK_1 d\theta_{\vec{K}_1} dK_{rs} \qquad (1)\end{aligned}$$

where ϕ_0 is the bistatic angle (see Fig. 1), $S(\cdot)$ is the ocean spectrum, $\vec{K}_1$ and $\vec{K}_2$ are ocean wave vectors of magnitude K_1, K_2 and direction $\theta_{\vec{K}_1}$, $\theta_{\vec{K}_2}$, respectively; ω_d is the Doppler frequency, K_0 is the radiation wavenumber, $\Delta\rho_{s21}$ is the patch width, $Sa(\cdot)$ is the sampling function, and $\delta(\cdot)$ is the delta function constraint. Γ_P is the so-called coupling coefficient which consists of the sum of an electromagnetic term (Γ_{EP}) and an hydrodynamic term Γ_H. It should be noted that $K_{rs} = |\vec{K}_1 + \vec{K}_2|$.

Using the relationship

$$\lim_{M\to\infty} Sa^2(Mx) = \pi\delta(x) \qquad (2)$$

is applied to (1), then

$$\begin{aligned}& \Delta\rho_{s21} Sa^2\left[\tfrac{\Delta\rho_{s21}}{2}\left(\tfrac{K_{rs}}{\cos\phi_0}-2K_0\right)\right]\\ =\;& 2\cos\phi_0\tfrac{\Delta\rho_{s21}}{2\cos\phi_0} Sa^2\left[\tfrac{\Delta\rho_{s21}}{2\cos\phi_0}\left(K_{rs}-2K_0\cos\phi_0\right)\right]\\ =\;& 2\pi\cos\phi_0\delta\left(K_{rs}-2K_0\cos\phi_0\right) \qquad (3)\end{aligned}$$

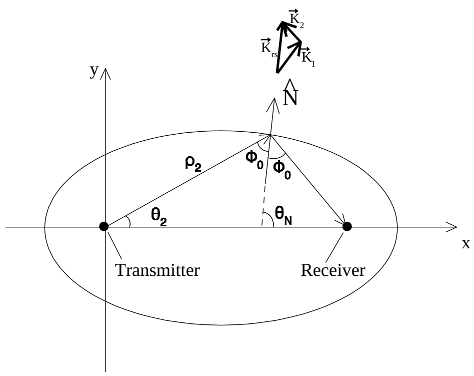

Fig. 1. Geometry of the bistatic scatter.

where $\Delta\rho_{s21} \to \infty$ is assumed. Inserting (3) into (1) and considering the property of the Dirac delta function gives

$$\begin{aligned}\sigma_{2P}(\omega_d) &= 2^6\pi^2 K_0^4 \sum_{m_1=\pm1}\sum_{m_2=\pm1}\int_{-\pi}^{\pi}\int_{-\infty}^{\infty} S(m_1\vec{K}_1) \\ &\cdot S(m_2\vec{K}_2)|\Gamma_P|^2 K_1 \cos^4\phi_0 \\ &\cdot\delta(\omega_d + m_1\sqrt{gK_1} + m_2\sqrt{gK_2})dK_1 d\theta_{\vec{K}_1} \quad (4)\end{aligned}$$

For backscattering, $\phi_0 = 0$ and (4) simplifies to

$$\begin{aligned}\sigma_{2P}(\omega_d) &= 2^6\pi^2 K_0^4 \sum_{m_1=\pm1}\sum_{m_2=\pm1}\int_{-\pi}^{\pi}\int_{-\infty}^{\infty} S(m_1\vec{K}_1) \\ &\cdot S(m_2\vec{K}_2)|\Gamma_P|^2 K_1 \\ &\cdot\delta(\omega_d + m_1\sqrt{gK_1} + m_2\sqrt{gK_2})dK_1 d\theta_{\vec{K}_1} \quad (5)\end{aligned}$$

Here, (5) is similar to Barrick's second-order cross section which is based on perturbation theory[2].

B. The Electromagnetic Coupling Coefficient

While the deep-water hydrodynamic coupling coefficient appears in all similar analyses (see, for example, [8]), the electromagnetic term differs. As a result of analysis similar to that found in [5], but opening the field convolutions as referred to above, the electromagnetic coupling coefficient for bistatic scatter in equations (4)–(5) is found to be

$$\Gamma_{EP} = \frac{-(\vec{K}_1\cdot\hat{\rho}_2)[\vec{K}_2\cdot(\vec{K}_1 - K_0\hat{\rho}_2)]}{K_{rs}\cos\phi_0\sqrt{\vec{K}_1\cdot(\vec{K}_1 - 2K_0\hat{\rho}_2)}} \quad (6)$$

Here $K_{rs} = 2K_0\cos\phi_0$ as dictated by the delta function in (3). The corresponding symmetrised monostatic result given by Walsh et al. [9] is

$${}_s\Gamma_{EP} = \frac{-j\left|\vec{K}_1\times\vec{K}_2\right|^2}{2K^2\sqrt{\vec{K}_1\cdot\vec{K}_2}} \quad (7)$$

where $K = 2K_0$, and $\vec{K}_1$, $\vec{K}_2$ is are equal to $\vec{K}_{mn}$ and $\vec{K}_{pq}$, respectively. (6) and (7) seem different from each other, but in fact they can be proved equivielent.

It is easy to show from the patch-scattering geometry that

$$\hat{\rho}_2 = \hat{x}\cos\theta_2 + \hat{y}\sin\theta_2 \quad (8)$$

can be written as

$$\hat{\rho}_2 = \hat{N}\cos\phi_0 + \hat{\theta}_N\sin\phi_0 \quad (9)$$

where the unit normal $\hat{N}$ and its orthogonal angular counterpart $\hat{\theta}_N$ may be written as

$$\begin{aligned}\hat{N} &= \hat{x}\cos(\theta_2+\phi_0) + \hat{y}\sin(\theta_2+\phi_0) \\ \hat{\theta}_N &= -\hat{x}\sin(\theta_2+\phi_0) + \hat{y}\cos(\theta_2+\phi_0) \quad (10)\end{aligned}$$

For backscattering ($\phi_0 = 0$),

$$\hat{\rho}_2 = \hat{N} \quad (11)$$

Then in (6), $\vec{K}_{rs} = 2K_0\cos\phi_0\hat{N} = 2K_0\hat{N}$. Dropping the rs subscript notation we simply write

$$\vec{K} = 2K_0\hat{N} \quad (12)$$

so that

$$\hat{\rho}_2 = \hat{N} = \frac{\vec{K}}{2K_0} = \hat{K}\ . \quad (13)$$

Furthermore,

$$\vec{K}_{mn} + \vec{K}_{pq} = \vec{K}_1 + \vec{K}_2 = 2K_0\hat{K} \quad (14)$$

Substituting (13)–(14) and $\phi_0 = 0°$ into (6),

$$\begin{aligned}\Gamma_{EP} &= \frac{-(\vec{K}_1\cdot\hat{K})[\vec{K}_2\cdot(\vec{K}_1 - K_0\hat{K})]}{K\sqrt{\vec{K}_1\cdot(\vec{K}_1 - 2K_0\hat{K})}} \\ &= \frac{-(\vec{K}_1\cdot\vec{K})[\vec{K}_2\cdot(2\vec{K}_1 - 2K_0\hat{K})]}{2K^2\sqrt{\vec{K}_1\cdot(-\vec{K}_2)}} \\ &= \frac{-[\vec{K}_1\cdot(\vec{K}_1+\vec{K}_2)][\vec{K}_2\cdot(\vec{K}_1-\vec{K}_2)]}{j2K^2\sqrt{\vec{K}_1\cdot\vec{K}_2}} \\ &= \frac{j[{K_1}^2 + K_1K_2\cos(\theta_{\vec{K}_1}-\theta_{\vec{K}_2})]}{2K^2\sqrt{\vec{K}_1\cdot\vec{K}_2}} \\ &\quad\cdot[K_1K_2\cos(\theta_{\vec{K}_1}-\theta_{\vec{K}_2}) - {K_2}^2] \\ &= \frac{-j\left|\vec{K}_1\times\vec{K}_2\right|^2}{2K^2\sqrt{\vec{K}_1\cdot\vec{K}_2}} + \frac{j\vec{K}_1\cdot\vec{K}_2({K_1}^2-{K_2}^2)}{2K^2\sqrt{\vec{K}_1\cdot\vec{K}_2}}\end{aligned} \quad (15)$$

Using the general "symmetrised" vector identity

$${}_s\Gamma_{EP}(\vec{K}_1,\vec{K}_2) = \frac{\Gamma_{EP}(\vec{K}_1,\vec{K}_2) + \Gamma_{EP}(\vec{K}_2,\vec{K}_1)}{2} \quad (16)$$

in (15) the coupling coefficience becomes

$$
{}_s\Gamma_{EP} = \frac{-j\left|\vec{K}_1 \times \vec{K}_2\right|^2}{2K^2\sqrt{\vec{K}_1 \cdot \vec{K}_2}} \tag{17}
$$

which is identical to (7). Therefore, the bistatic radar cross section of equation (1) properly reduces in all respects to the existing monostatic models.

III. Inversion of the Bistatic Cross Section of Patch Scatter

Based upon the second-order HF bistatic radar cross section above, an algorithm for the inverse problem of recovering the non-directional ocean wave spectrum from sea echo (patch scatter) for various wind speeds and directions is addressed.

A. Normalized Second-order Cross Section

As suggested by previous investigators (eg., [8], [10]–[11]) who addressed the monostatic problem, the bistatic cross section may be normalized to simplify the computation work. The main normalizing factor for the bistatic cross sections, in keeping with the associated monostatic case, is chosen to be $2K_0\cos\phi_0$. Then, the normalized first- and second-order bistatic cross sections $\sigma_{1n}(\eta)$ and $\sigma_{2Pn}(\eta)$ can be expressed as

$$
\begin{aligned}
\sigma_{1n}(\eta) &= 2^3\pi K_0 \Delta\rho_s \sum_{m=\pm 1} Z_1(m\vec{K}_n) K_n^{\frac{5}{2}} \\
&\quad \cdot Sa^2\left[\Delta\rho_s K_0\left(K_{rsn}-1\right)\right]
\end{aligned} \tag{18}
$$

and

$$
\begin{aligned}
\sigma_{2Pn}(\eta) &= 2^2\pi^2 \sum_{m_1=\pm 1}\sum_{m_2=\pm 1}\int_{-\pi}^{\pi}\int_0^{\infty} Z_1(m_1\vec{K}_{1n}) \\
&\quad \cdot Z_1(m_2\vec{K}_{2n})|\Gamma_{Pn}|^2 K_{1n} \\
&\quad \cdot \delta\left(\eta + m_1\sqrt{K_{1n}} + m_2\sqrt{K_{2n}}\right) dK_{1n} d\theta_{\vec{K}_{1n}}
\end{aligned} \tag{19}
$$

where $Z(\cdot)$, η, and Γ_{Pn} are the normalized versions of the ocean spectrum, the Doppler frequency (normalized to the Bragg frequency) and the coupling coefficient, respectively. While Γ_{Pn} has both hydrodynamic and electromagnetic terms, only the former, denoted as Γ_{Hn}, is dominant in the region of interest. It alone is considered in the inverse problem here. That is,

$$
\begin{aligned}
\Gamma_{Hn} &= \frac{1}{2}\left[K_{1n} + K_{2n}\right. \\
&\quad \left. + \frac{K_{1n}K_{2n} - \vec{K}_{1n}\cdot\vec{K}_{2n}}{m_1 m_2\sqrt{K_{1n}K_{2n}}}\left(\frac{1+\eta}{1-\eta}\right)\right]
\end{aligned} \tag{20}
$$

The delta function constraint may be calculated by means of the Newton-Raphson method. This reduces the dual integral equation to a single integration. The values of K_{1n} and K_{2n} for each η and $\theta_{\vec{K}_{1n}}$ are derived. The result is given by

$$
\begin{aligned}
\sigma_{2Pn}(\eta) &= 2^3\pi^2 \sum_{m_1=\pm 1}\sum_{m_2=\pm 1}\int_{-\pi}^{\pi} Z_1(m_1\vec{K}_{1n}) \\
&\quad \cdot Z_1(m_2\vec{K}_{2n})|\Gamma_{Pn}|^2 J_{tn} K_{1n}^{\frac{3}{2}} d\theta_{\vec{K}_{1n}} .
\end{aligned} \tag{21}
$$

The factor J_{tn} is a normalized version of the required Jacobian transformation and has the form

$$
J_{tn} = \left|1 + m_1 m_2 \frac{Y_{1n}^3 - Y_{1n}\cos(\theta_{\vec{K}_{1n}} - \theta_N)}{[1 + Y_{1n}^4\cos(\theta_{\vec{K}_{1n}} - \theta_N)]^{\frac{3}{4}}}\right|^{-1} \tag{22}
$$

where $Y_{1n} = \sqrt{K_{1n}}$.

B. Matrix Equation and SVD Method

The next step of the inversion is to linearize the integral equation. The non-linearity of the integrand comes from the product of two unknown, but related factors, $Z_1(m_1\vec{K}_{1n})$ and $Z_1(m_2\vec{K}_{2n})$, the normalized ocean wave directional spectra. Each of them may be viewed as the combination of a nondirectional spectrum and a cardioid directional factor, and may be represented by a truncated Fourier series whose sin terms, from symmetry, are zero. Using a's to represent the remaining Fourier coefficients

$$
\begin{aligned}
&Z_1(m_1\vec{K}_{1n})Z_1(m_2\vec{K}_{2n}) \\
&\quad = \frac{1}{4\pi^2}\cdot\sum_{p=0}^{2}\sum_{q=0}^{2}\left[a_p(K_{1n})\cos(p\theta_{\vec{K}_{1n}})\right] \\
&\quad \cdot\left[a_q(K_{2n})\cos(q\theta_{\vec{K}_{2n}})\right]
\end{aligned} \tag{23}
$$

A common linearization (see, for example, Gill [10]) used to simplify the nonlinear product is obtained by setting

$$
a_q(K_{2n}) = \frac{a_q(K_B)}{K_{2n}^4} \tag{24}
$$

where $K_B = 1$ is the normalized Bragg wavenumber and $a_q(K_B)$ may be derived from the first-order cross section.

After the linearization, the second-order bistatic cross section, $\sigma_{2PnL}(\eta)$, may be rewritten as

$$
\sigma_{2PnL}(\eta) = 2\sum_{m_1=\pm 1}\sum_{m_2=\pm 1}\sum_{p=0}^{2}\sum_{q=0}^{2}\int_{\theta_{\vec{K}_{1n}}} C_{pq}a_p(K_{1n})d\theta_{\vec{K}_1} \tag{25}
$$

where the factor C_{pq} is given by

$$
C_{pq} = a_q(K_B)\cos(p\theta_{\vec{K}_{1n}})\cos(q\theta_{\vec{K}_{2n}})|\Gamma_{Pn}|^2 J_{tn}\frac{K_{1n}^{\frac{3}{2}}}{K_{2n}^4} . \tag{26}
$$

The integral equation may then be discretized to the form

$$
\underline{\underline{A}}\,\underline{X} = \underline{B} \tag{27}
$$

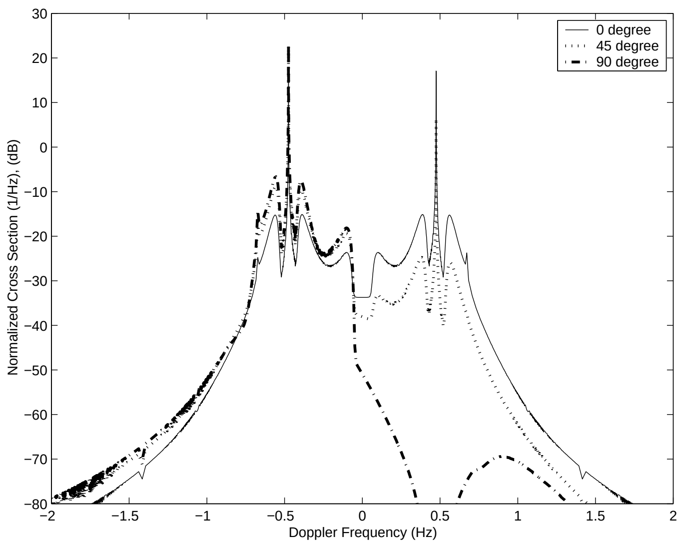

Fig. 2. Bistatic patch scatter Doppler spectra under different wind directions with wind speed of 15 m/s.

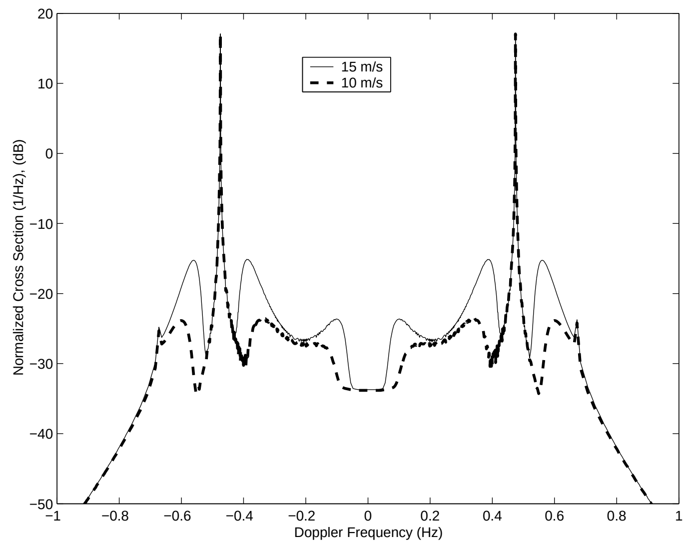

Fig. 3. Bistatic patch scatter Doppler spectra for different wind speeds with wind direction of 0°.

where $\underline{\underline{A}}$ is denoted as the kernel matrix. The rows of the kernel matrix are arranged corresponding to the selected normalized frequencies, while the columns correspond to frequency bands. $\underline{B}$ is a column array with the number of its elements being the same as the rows of $\underline{\underline{A}}$. $\underline{X}$ is a column matrix corresponding to the Fourier coefficients. The non-directional ocean wave spectrum $F(K)$ may be recovered from the Fourier coefficient $a_0(K_{1n})$.

$$F(K) = \frac{\pi}{2} a_0(K) \ . \tag{28}$$

Equation (27) is "solved" by means of a singular value decomposition (SVD) and uses $\underline{\underline{A}}^{+}$ as the pseudo-inverse of $\underline{\underline{A}}$. That is,

$$\underline{X} \approx \underline{\underline{A}}^{+} \underline{B} \tag{29}$$

with

$$\underline{\underline{A}}^{+} = \underline{\underline{V}} \begin{bmatrix} \Sigma^{-1} & \dots & 0 \\ \vdots & \ddots & \vdots \\ 0 & \dots & 0 \end{bmatrix} \underline{\underline{U}}^{T} \tag{30}$$

where Σ is the diagonal matrix containing the singular values of $\underline{\underline{A}}$ and Σ^{-1} is the inverse of Σ. $\underline{\underline{U}}$ and $\underline{\underline{V}}$ are orthogonal matrices. $\underline{\underline{U}}^{T}$ is the transpose of U.

IV. Simulation Results

The radar cross section, normalized to patch area, is modelled using the Pierson-Moskowiz model [12] with a cardiod directional distribution for the directional ocean wave height spectrum of a wind driven sea. Samples of the bistatic second-order radar cross section for deep water patch scatter are computed and plotted by using the relationships in Section II. An operating frequency of 25 MHz, a bistatic angle of 30°, an ellipse normal angle of

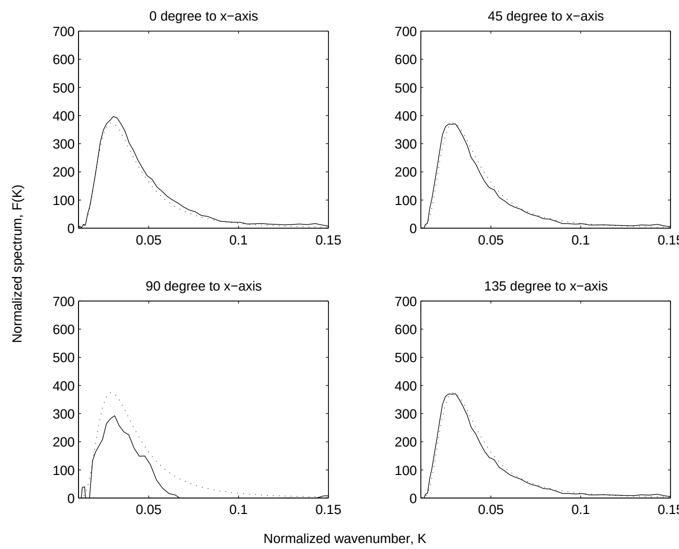

Fig. 4. The recovered normalized non-directional ocean wave spectra for four wind directions. The parameters are chosen associated with Fig. 2. The dotted-lines are the original spectra, and the solid-lines are the simulated results.

90°, and a patch width of 2 km were chosen for illustrative purposes. Fig. 2. shows the result under different wind directions for a wind speed of 15 m/s. The wind direction is referenced to the x axis (see Fig. 1). The cross sections are given in

terms of Doppler frequency and are plotted on a decibel scale. Fig. 3. shows the effect of wind speed on the Doppler spectrum for a wind direction of 0°.

Fig. 4 and Fig. 5 depict the results of inversion from Fig. 2 and Fig. 3. Under these conditions, the measured ocean wave frequency is approximately from 0.065 Hz to 0.231 Hz. For the wind speeds considered, this range of frequency contains the bulk of the ocean wave energy.

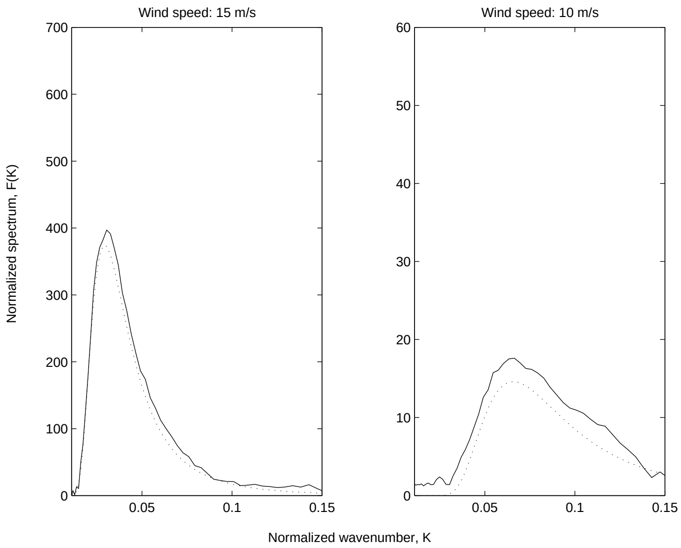

Fig. 5. The recovered non-directional ocean wave spectra for two wind speeds. The parameters are chosen associated with Fig. 3. The dotted-lines are the original spectra, and the solid-lines are the simulated results.

Note from Fig. 5 that, as expected, the results for wind directions of 45° and 135° are identical.

V. Concluding Remarks

In this paper, the development of a model for the ocean patch scatter for bistatic radar is documented. An algorithm also is developed to invert the bistatic cross section of the patch scatter. The recovered non-directional ocean wave spectra for different wind directions and speeds are plotted. The results from simulations are encouraging and future work is planned for field data to be derived from radars on the Canadian East Coast.

Acknowlegements

This work was supported by a Natural Sciences and Engineering Research Council of Canada grant (NSERC 238263-01) to Dr. E. Gill.

References

[1] D.E. Barrick, "First-order theory and analysis of MF/HF/VHF scatter from the sea", *IEEE Trans. Antennas Propagat.*, vol. 20, pp. 2–10, 1972.

[2] D. Barrick, "Remote sensing of sea state by radar", in *Remote Sensing of the Troposphere*, V.E. Derr, Ed., chapter 12, pp. 1–46. U.S. Government Printing Office, Washington, DC, 1972.

[3] Gill, E. and J. Walsh, "A perspective on two decades of fundamental and applied research in electromagnetic scattering and high frequency ground wave radar on the Canadian east coast", Proc.IGARSS 2002, Toronto, Canada, May, 2002.

[4] E.W. Gill, and J.Walsh, "Bistatic form of the electric field equations for the scattering of vertically polarized high-frequency ground wave radiation from slightly rough, good conducting surfaces", *Radio Science.*, vol. 35, pp. 1360–10, 2000.

[5] E.W. Gill, and J.Walsh, "High-frequency bistatic cross sections of the ocean surface", *Radio Science.*, vol. 36, pp. 1360–10, 2001.

[6] Lipa, B.J. and D.E. Barrick, "Extraction of sea state from HF radar sea echo: Mathematical theory and modeling", *Radio Science.*, vol. 21, no. 1, pp 81-100, 1986.

[7] E. Gill, and J. Walsh, "On the second-order high frequency bistatic ground wave radar cross section of the ocean surface," in *Proc. IEEE Canadian Conference on Electrical and Computer Engineering*, St. Johns, Newfoundland, Canada, 1997.

[8] B.J. Lipa and D.E. Barrick, "Analysis Methods for Narrow-beam High-frequency Radar Sea Echo", Technical Report ERL 420-WPL 56, National Oceanic and Atmospheric Administration, U.S. Department of Commerce, pp. 54, 1982.

[9] J.Walsh, R. Howell, and B. Dawe, "Model development for evaluation studies of ground wave radar", contract report 90-C14, Cent. for Cold Ocean Resour. Eng., Mem. Univ. of Newfoundland, St. John's, Newfoundland, Canada, 1990.

[10] E. Gill and J. Walsh, "Extraction of ocean wave parameters from HF backscatter received by a four-element array: Analysis and application", *IEEE J. Oceanic Eng.*, vol. 17, no. 4, pp. 376-386, 1992.

[11] R. Howell and J. Walsh, "Measurement of ocean wave spectra using narrow beam HF radar", *IEEE J. Oceanic Eng.*, vol. 18, no. 3, pp. 296-305, 1993

[12] Pierson, W., and L. Moskowiz, "A proposed spectral form for fully developed seas based upon the similarity theory of S.A. Kitaigorodskii", *J. Geophys. Res.*, vol. 69, pp. 5181–5190, 1964.